JOURNAL OF MATERIALS SCIENCE 25 (1990) 3191–3198

Titanium-base coating on plane silica substrates

R. HILLEL*, M. P. BERTHET, J. BOUIX
Laboratoire de Physicochimie Minérale, (CNRS, UA 116), France
A. ROCHE
Département de Chimie Appliquée et Génie Chimique, CNRS, UA 417, Université Claude Bernard, Lyon 1, 69622 Villeurbanne Cedex, France

Plane silica substrates were coated with a titanium-based deposit by gaseous cementation at temperatures ranging from 600 to 800° C, over 1 h to several tens of hours. The cement consisted of hydrogen chloride and titanium. The bilayer structure of the coating was established by X-ray diffraction, X-ray electron microprobe analysis, scanning electron microscopy, low-energy electron-induced X-ray spectroscopy, X-ray photoelectron spectroscopy, optical microscopy and X-ray fluorescence spectroscopy. Thin coatings were amorphous and the composition of the outer zone was close to TiO. Thicker coatings ranging from 2 to 30 μm were crystalline. In this case, the outer layer, designated α-Ti(O) or TiO_x with $0.44 \leqslant x \leqslant 0.49$, corresponded to an ordered solid solution of oxygen in a close-packed hexagonal titanium. The inner layer in contact with the substrate was Ti_5Si_3. At fixed temperatures (600, 650, 700, and 800° C), the thickness of the coating increased according to a parabolic law. Activation energy and diffusion coefficient were calculated. Thermodynamic considerations concerning the interactions between the gaseous phase of cementation and the silica substrate, are presented from theoretical calculations and from Ti–Si–O phase diagrams experimentally constructed at 800, 1000 and 1300° C.

1. Introduction

A titanium-based coating treatment for ceramic oxide substrates has been developed. The aim of the present work was to study the behaviour of as-coated substrates embedded within an aluminium or titanium matrix. It is expected that this type of coating will work as an interphase allowing protection of the ceramic oxides against metallic attacks at high temperatures, i.e. acting as a diffusion barrier to prevent the possible formation of brittle layers. On the other hand, a greater substrate–matrix adhesion, due to the existence of some chemical reaction between the coating and aluminium or titanium, is still under consideration.

In the present investigation we studied a titanium-based coating on plane silica substrates. The coating method is first presented. The chemical and microstructural properties of the titanium-based coating are described. Finally, some characteristics of the kinetics and some thermodynamic considerations of the coating growth are given.

2. Titanium-based coating method

Plane silica substrates (α-quartz; optical quality; 10 mm × 10 mm thickness 1 mm) were treated by gaseous cementation in silica; 2 ampoules (internal diameter 10 mm; length 60 mm). The cement consisted of hydrogen chloride (99.0 wt % purity), and thin sheets of titanium (10 mm × 2 mm; thickness 0.2 mm; 99.6 wt % purity) solvent degreased, etched in a fluoro-nitro-ammoniaco solution, rinsed and dried under vacuum. The HCl concentration was equal to 1.07×10^{-5} mol cm^{-3} and the quantity of titanium corresponded to the atomic ratio Ti/Cl = 100. The silica substrates were ultrasonically degreased in alcohol, acetone, rinsed and dried. The ampoules were filled with the cement and the plane silica substrates in such a way that the substrates were not in contact with titanium. The ampoules were sealed and heated in the temperature range 600 to 800° C in a resistance furnace. The treatment times were in the range 1 to 200 h. After cooling, the ampoules were broken and the samples were ultrasonically cleaned in acetone. According to the temperature and time, the colour of the coating varied from iridescent brown to black mirror and finally to metallic grey. At 600° C, these three colourings were obtained after 2 h treatment, less than 50 h and more than 50 h, respectively. At 700° C, the black mirror colour was obtained when the time did not exceed 5 h. At temperatures higher than 800° C, the metallic grey colouring was always obtained. Up to 700° C, even for long durations, the coatings appeared to be tightly bonded to the silica substrate, whereas at 800° C the coating became poorly adherent when the duration exceeded 50 h. We will see later that the metallic grey colour of the coatings is correlated with the crystalline phases.

3. Titanium-based coating analysis

In order to characterize the titanium-based coatings, several complementary techniques have been used: X-ray diffraction (XRD), X-ray electron microprobe

* *Present address*: IMP-CNRS, Universite, 66025, Perpignan Cedex, France.

0022–2461/90 $03.00 + .12

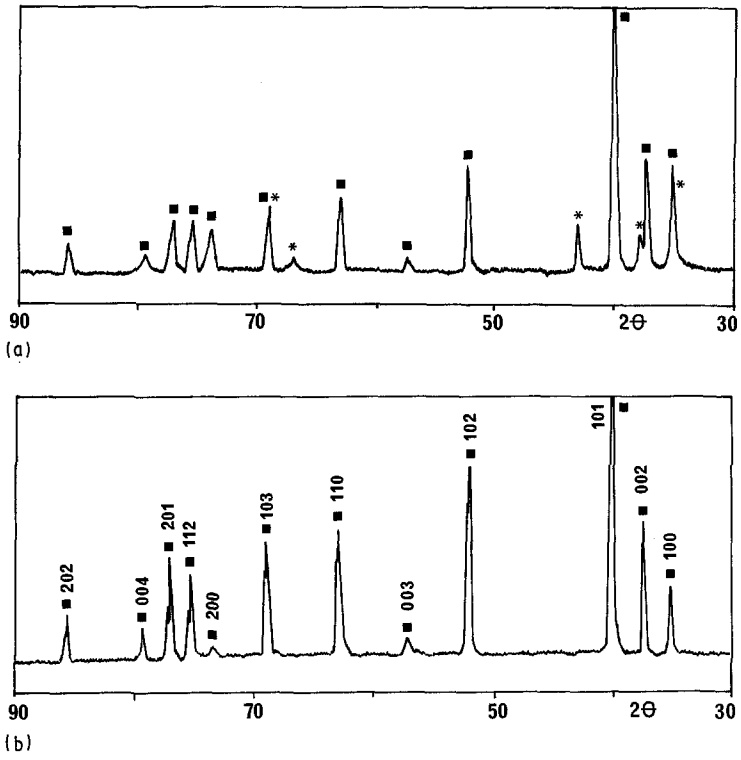

Figure 1 X-ray diffraction patterns of: (a) a silica substrate coated at 824° C for 4 h, (b) a standard powder $TiO_{0.5}$. (■) X-ray diffraction lines attributed to α-Ti(O); (*) X-ray diffraction lines attributed to Ti_5Si_3.

analysis (EMPA), scanning electron microscopy (SEM), low-energy electron induced X-ray spectroscopy (LEEIXS), X-ray photoelectron spectroscopy (XPS), optical microscopy, and X-ray fluorescence spectroscopy (XRFS).

3.1. XRD

X-ray diffraction analyses were performed with a Philips PW 1840 diffractometer using nickel-filtered copper radiation. The X-ray diffraction lines (Fig. 1) were ascribed to two phases: Ti_5Si_3 and TiO_x with $x \leqslant 0.5$. The latter phase, designated α-Ti(O), corresponds to a solid solution of oxygen in titanium, with oxygen occupying interstitial positions in the close-packed hexagonal lattice of titanium. The presence of α-Ti(O) was supported by comparing the X-ray diffraction patterns of the coated substrates with that of a standard powder of $TiO_{0.5}$ prepared and analysed by Garnier [1]. It was established [2, 3] that $TiO_{0.5}$ corresponds to the maximum solubility of oxygen within the hexagonal close-packed structure of titanium. In Fig. 1 the X-ray diffraction spectra of $TiO_{0.5}$ and of a silica substrate treated at 824° C for 4 h are given. We observe that most of the lines of the coated sample differ from those of $TiO_{0.5}$ in a slight shift towards large angles. The same patterns were registered with the other samples covered by a thick coating (thickness $\geqslant 2\,\mu m$), but this shift varied with the treatment conditions. We have interpreted all these lines as a hexagonal structure and calculated the values of the lattice parameters a and c from the measured X-ray diffraction lines, using a least squares procedure. These values ranged from 0.2962 to 0.2968 nm for a and from 0.4783 to 0.4844 nm for c. We conclude that the compound formed was a solid solution of oxygen in titanium and that the shift corresponded to the evolution of the lattice parameters with the oxygen concentration.

We determined the oxygen concentration of this phase graphically for each crystalline-coated substrate using the fitted lines presented in Fig. 2. These lines were established using the lattice parameter data as a function of oxygen/titanium atomic ratio, given by several authors [2–8] (68 sets of data). Although some discrepancies exist between a couple of the a and c values determined from these two lines, we consider that the mean values were representative of the oxygen amount. These results are used to represent the treatment time effect on the O/Ti atomic ratio for

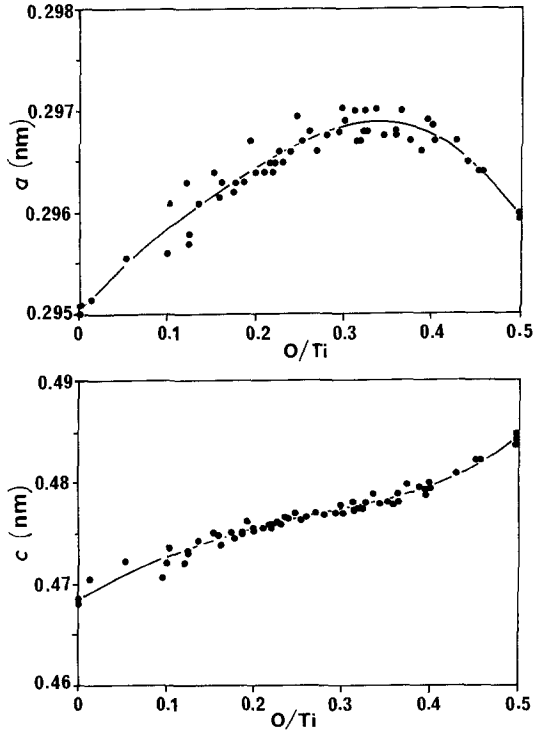

Figure 2 Fitted lines established from the literature values of the α-Ti(O) hexagonal lattice parameters a and c (nm) as a function of oxygen composition.

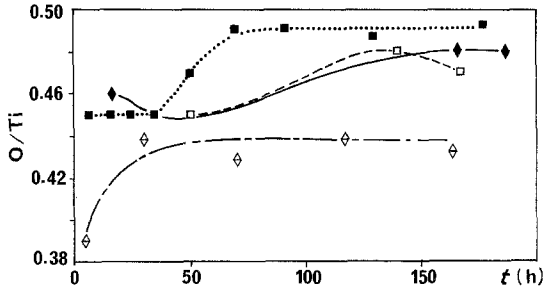

Figure 3 Evolution of the atomic ratio O/Ti of the α-Ti(O) phase with treatment time. (□) 600° C, (◆) 650° C, (■) 700° C, (◈) 800° C.

coating temperatures 600, 650, 700, and 800° C. Fig. 3 shows that for crystalline coatings, the O/Ti atomic ratio determined graphically from Fig. 2, slowly increases with the treatment time and reaches limit values ranging from 0.44 to 0.49. These atomic ratio values were assumed to be representative of the whole Ti–O crystalline phase, from the fact that the coating thicknesses were thinner than the penetration depth of the X-rays. In fact, we assumed that the limit of the analysed depth, x, could be evaluated from the absorption law $\ln(I_0/I) = \rho\mu x$ with $I_0/I = 100$. Using the $TiO_{0.5}$ density, $\rho = 5.05\,g\,cm^{-3}$ [2], and the $TiO_{0.5}$ mass absorption coefficient, μ, for CuKα radiation $= 184\,cm^2\,g^{-1}$ [9], we found $x = 49\,\mu m$, whereas, as we will see further, the coating thicknesses do not exceed $30\,\mu m$ under our conditions.

It is well known [2–4, 6] that the points at O/Ti = 0.33 (Fig. 2) correspond to a transition from a random distribution of oxygen in the composition range $0 <$ O/Ti < 0.33 (hexagonal lattice P63/mmc, no. 194) to an ordered arrangement (hexagonal lattice P3 m1, no. 164), $TiO_{0.5}$ being the phase boundary on the oxygen side. In the ordered phases, two extra lines, 0 0 1 and 0 0 3, are allowed. In fact, under our conditions, the (0 0 1) reflection was not observed even in $TiO_{0.5}$ powder, whereas a very weak (0 0 3) reflection was detected (Fig. 1).

The X-ray diffraction lines corresponding to Ti_5Si_3 (Fig. 1): $d_{002} = 0.2571$, $d_{012} = 0.2390$, $d_{112} = 0.2119$, d_{123} or $d_{140} = 0.1405$, and $d_{042} = 0.1368$ nm, were assigned by comparison with those listed in the JCPDS (no. 29-1362). The position of these diffraction lines are constant, agreeing with the fact that the homogeneity range of the Ti_5Si_3 phase is narrow (4% about stoichiometry [10]). However, as this phase has some common lines with α-Ti(O), the identification was ambiguous and required complementary analyses.

3.2. EMP analysis

X-ray electron microprobe analyses were done in a semi-automated Cameca model microprobe equipped with energy dispersive X-ray spectrometer (Tracor TN 2000). They were achieved on polished cross-sections of substrates embedded in resin and carbon-coated. The spot diameter of the electron beam was about $1\,\mu m$. An operating voltage of 10 kV, a beam current of 8 to 9 nA and a counting interval of 20 sec were selected. According to the spot size of the electron beam, point count determinations of Si$K\alpha$ and Ti$K\alpha$ were done at $1.25\,\mu m$ intervals across the interfacial zone. Because oxygen is too light for this kind of analysis, its concentration was given by the difference, after having verified its presence by wavelength dispersive X-ray spectrometry. When titanium and oxygen were present together, the microprobe data were corrected using TiO and TiO_2 single crystals as standards. When titanium and silicon were present with a small quantity of oxygen, the microprobe data were corrected using $TiSi_2$ single crystal and fused polycrystalline Ti_5Si_3 as standards. The results obtained with a silica substrate treated at 650° C for 74 h and giving a crystalline coating, indicate three distinct regions (Fig. 4): a titanium oxide layer and a titanium silicide layer corresponding to the coating, and the SiO_2 substrate. The composition of the Ti–O outer layer is about $TiO_{0.5}$, that is in agreement with the previous X-ray determinations (Fig. 3). In the inner layer, the mean value (1.68) of the atomic ratio Ti/Si is close to 1.67, corresponding to Ti_5Si_3. In this phase, oxygen is present with an atomic per cent of about 13. The whole thickness of the coating is about $6\,\mu m$, corresponding to about $4\,\mu m$ for the titanium oxide layer and $2\,\mu m$ for the titanium silicide layer.

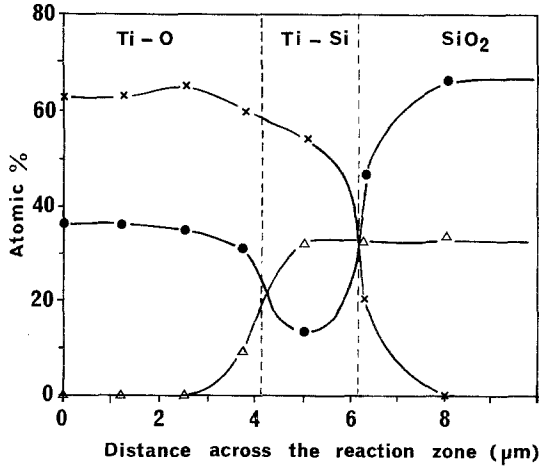

Figure 4 X-ray electron microprobe elemental profiles of the elements (×) Ti, (△) Si, and (●) O in the reaction zone of a substrate coated at 650° C, 74 h.

X-ray maps (Si$K\alpha$ and Ti$K\alpha$) of coated substrate cross-sections presented in Fig. 5 show homogeneous coating with a double-layer structure and corresponding to the α-Ti(O) and Ti_5Si_3 phases.

3.3. LEEIXS analysis

The low-energy electron-induced X-ray spectroscopy developed in the Applied Chemistry Department, University Claude Bernard, has been extensively described elsewhere [11, 12]. The Ti$L\alpha$, β emission band has been recorded with an electron beam energy of 3 keV and an electron current density of $0.3\,mA\,cm^{-2}$ for standards (Fig. 6) and titanium-based coatings (Fig. 7). The analysing crystal used was a natural clinochlore {(0 0 1), ($2d = 2.839$ nm)}. A 90° take off specimen holder was used. According to the Feldmann relationship [11], and assuming a TiO-like oxide layer ($\rho = 5.89\,g\,cm^{-3}$; JCPDS no. 23-1078), the probe thickness is about 70 nm. The fine structures of the Ti$L\alpha$, β emission band and their energy shift are

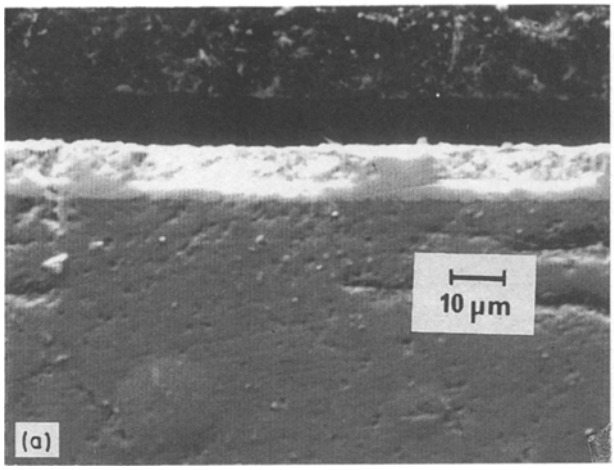

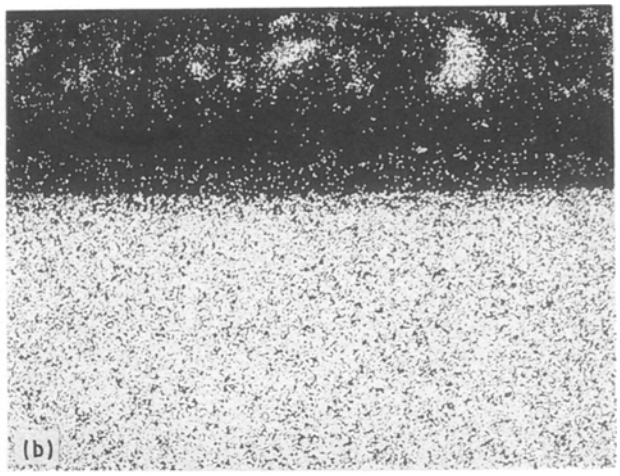

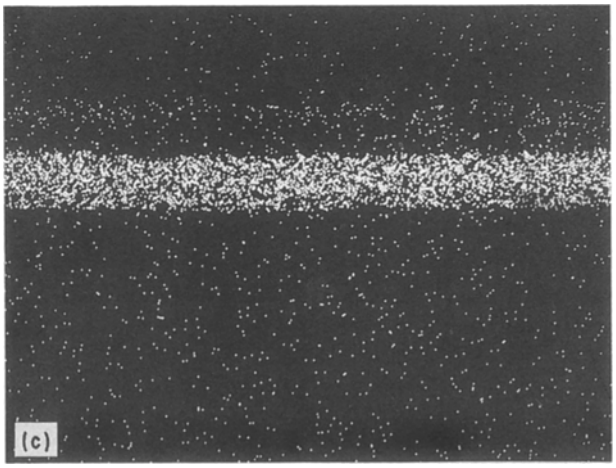

Figure 5 (a) Scanning electron micrograph and X-ray maps (b) Si$K\alpha$ and (c) Ti$K\alpha$ of cross-sections of a substrate coated at 700° C for 112 h.

characteristic of the various chemical bondings of titanium. Standard spectra are in good agreement with those obtained by Baun [13]. It can be easily observed that for the thin amorphous coatings, Ti$L\alpha$, β spectra are similar to TiO-like oxide phase with TiO_2 at the surface (i.e. 590° C, 1/2 h). For the thicker crystalline coatings, the fine structure of the Ti$L\alpha$, β spectra are similar to that obtained with $TiO_{0.5}$-like oxide.

3.4. XPS analysis

For reaction zones thinner than 2 μm, X-ray photoelectron spectroscopy has been used (Hewlett-Packard HP 5950 A electron spectrometer with Al$K\alpha$ radiation) and elemental sputter profiles were obtained by recording the intensity of the photopeaks of Ti, Si, and O ($Ti2p_{3/2}$ and $Ti2p_{1/2}$; Si2p; O1s) after sample sputtering in a preparation vessel. Under our experimental conditions, we assumed that the sputtering rate was independent of the nature of the different layers. An average rate for such a coating of about 0.05 nm $mA^{-1}\,min^{-1}$ was evaluated with a talistep instrument (Tencor Instrument). Under these conditions, the profile step was about 10 nm, allowing the analysis of reaction zone thicknesses of about 100 nm and more. The in-depth profiles obtained with two samples treated

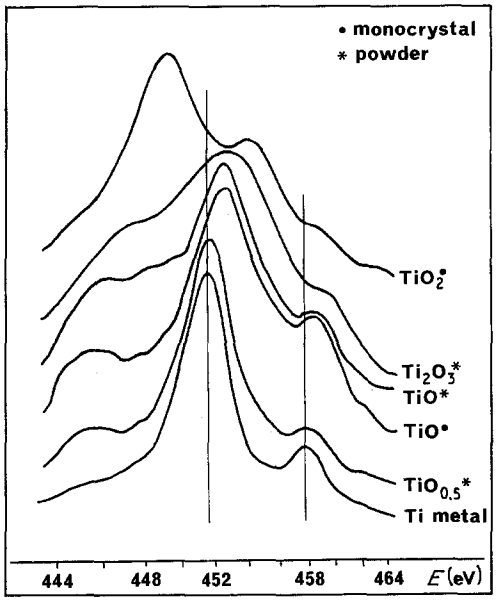

Figure 6 Ti$L\alpha$, β spectra of standard titanium oxide compounds obtained by LEEIXS.

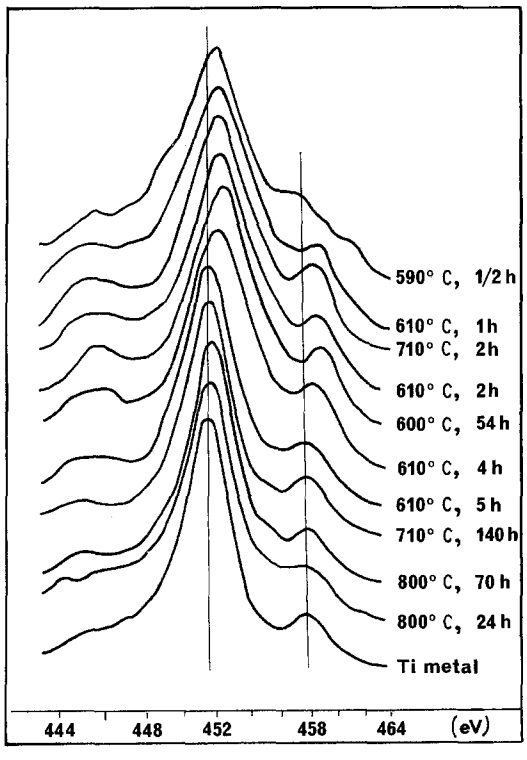

Figure 7 Ti$L\alpha$, β spectra of titanium-based coatings obtained by LEEIXS.

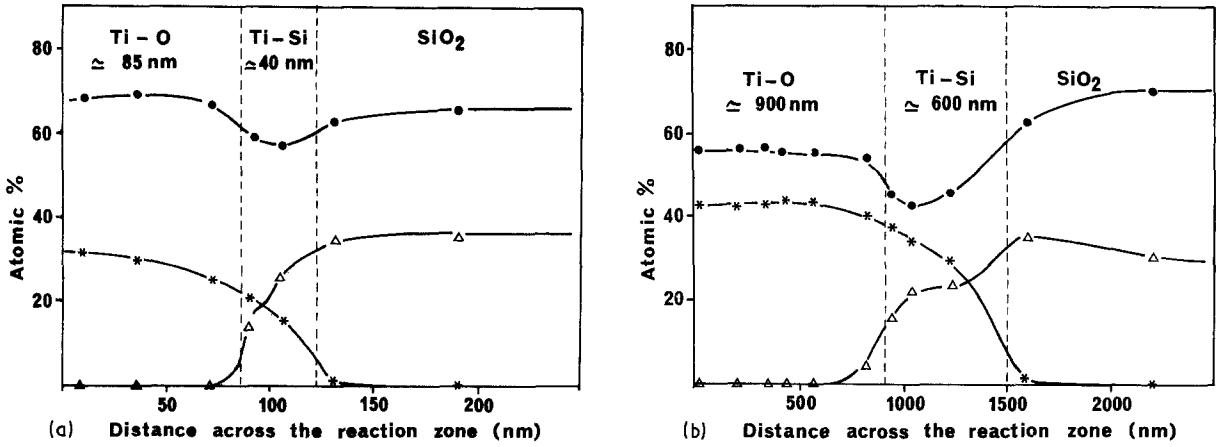

Figure 8 XPS depth profiles of (*) Ti, (△) Si, and (●) O, for two coated substrates: (a) 600° C, 1 h; (b) 600° C, 50 h.

at 600° C, 50 h and 600° C, 1 h (Fig. 8) show that three phases are still present, even in the case of amorphous coatings, and distributed in the reaction zone in a similar manner as in thick coatings. The outer zone is a titanium oxide phase and the inner layer is a titanium silicide-type compound where oxygen is still present. In the thinner coating whose thickness is about 150 nm (Fig. 8a), there is a surface layer corresponding to an atomic ratio Ti/O of about 2 and whose $Ti2p_{3/2}$ chemical shift Δ(Ti), is close to that of TiO_2 (Table I). The inner layer is made up of Ti, Si, and O and its Δ(Ti) approaches zero. In the thicker coating (Fig. 8b) but still amorphous (thickness less than 1.5 μm), the composition and the Δ(Ti) of the outer zone correspond to those of TiO [14] (Table II). From the Ti, Si and O atomic per cent and the Δ(Ti) values of the inner layer, the presence of both titanium silicide and suboxide titanium phases can be assumed. These results are in good agreement with those obtained by the LEEIXS technique.

4. Growth kinetics of the titanium-based coating

In addition to scanning electron micrographs and X-ray maps (Fig. 5), optical micrographs (Olympus, Vanox-T) (Fig. 9) show that for thick coatings the reaction zone usually has a regular contour. Therefore, we considered that it was possible to use the mean thickness of the coating as a basis for kinetics study. Thickness measurements were performed by optical microscopy, on polished cross-sections of coated substrates embedded in resin. The mean thicknesses larger than 2 μm were determined using an image analyser procedure (Olympus Corporation, C-2). We evaluated thicknesses smaller than 2 μm using X-ray fluorescence spectroscopy. According to the thin film approximation, we assumed that the intensity of the Ti*Kα* emission line was proportional to the thickness of the titanium-based coating. As shown in Fig. 10, the thickness of the coating, y, increases linearly with the square root of the treatment time, t, at a given

TABLE I XPS analysis of a titanium-based coated silica substrate at 600° C, 1 h. Binding energies (eV) of the $Ti2p_{3/2}$, Si2p, O1s photopics and titanium chemical shifts are shown as a function of the analysed depth. (The photopic $Ti2p_{3/2}$ of the titanium metal and the photopic of the polluting carbon were positioned at 453.8 [14] and at 285 eV, respectively)

Analysed depth (nm)	$Ti2p_{3/2}$ (±0.2 eV)	O1s (±0.2 eV)	Si2p (±0.2 eV)	$\Delta(Ti2p_{3/2}-Ti2p_{3/2metal})$ (±0.4 eV)
0	458.8	530.4	–	5.0
10	458.8	530.8	–	5.0
35	459.1	530.9	–	5.3
105	454.9	531.0	103.7	1.1
130	454.3	532.2	103.1	0.5

TABLE II XPS analysis of a titanium-based coated silica substrate at 600° C, 50 h. Binding energies (eV) of the $Ti2p_{3/2}$, Si2p, O1s photopics and titanium chemical shifts are shown as a function of the analysed depth

Analysed depth (nm)	$Ti2p_{3/2}$ (±0.2 eV)	O1s (±0.2 eV)	Si2p (±0.2 eV)	$\Delta(Ti2p_{3/2}-Ti2p_{3/2metal})$ (±0.2 eV)
30	455.4	531.2		1.6
210	455.3	531.2		1.5
330	455.2	531.2		1.4
420	455.6	531.9		1.8
570	454.9	531.6		1.1
820	454.7	531.7	99.0	0.9
940	454.4	531.5	98.8	0.6
1030	454.6	531.7	98.9/103.8	0.8
1220	454.5	531.2/532.8	98.9/103.6	0.7
1585	453.3	532.6	103.1	0
2185		532.8	103.4	

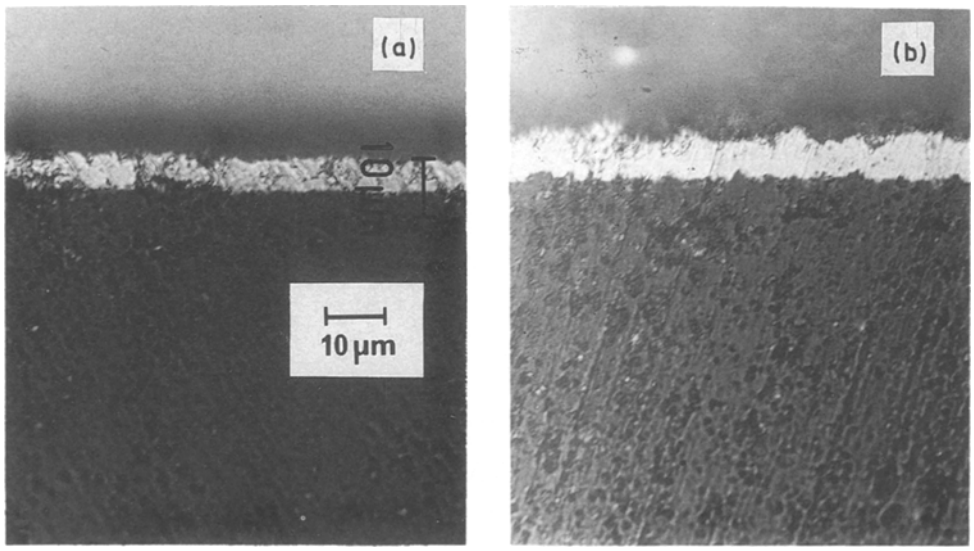

Figure 9 Optical micrographs of cross-sections of coated substrates at (a) 650° C, 74 h and (b) 700° C, 50 h.

temperature (600, 650, 700, and 800° C), i.e. consistent with a diffusion-limited growth and at least in a first approximation, $y^2 = k.\ t$, where k is the diffusion coefficient. The thermal variations of the diffusion coefficient follow an Arrhenius law: $k = k_o \exp(-E_a/RT)$, where E_a is the activation energy. $E_a = 147.6\,kJ\,mol^{-1}$ and $k_o = 1.969 \times 10^{-4}\,cm^2\,sec^{-1}$ were determined by plotting as a function of reciprocal of absolute temperature, for four values of k calculated from the slope squares of the $y = f(t1/2)$ straight lines (Fig. 10).

5. Thermodynamics of the titanium-based coating growth

As is often the case for phenomena controlled by diffusion, the reaction zone phases α-Ti(O) and Ti_5Si_3 are in metastable equilibrium with SiO_2. This is illustrated by the Ti–Si–O ternary phase diagrams presented in Fig. 11. We previously determined experimentally the drawn tie lines from the observed titanium–silica reactions occurring at 800, 1000 and 1300° C [15].

At 800° C, for SiO_2-poor initial mixtures, this compound was almost entirely converted into two phases (Fig. 11a): the titanium silicide Ti_5Si_3 and a solid solution of oxygen in a close-packed hexagonal titanium, TiO_x with $x \leqslant 0.5$, designated α-Ti(O). For SiO_2-rich mixtures, part of this compound was recovered with the reaction products Ti_2Si_3 and TiO_x with x tending to reach a maximum value of 0.5.

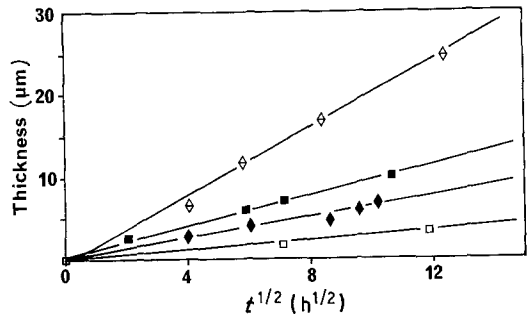

Figure 10 Variation of the coating thickness as a function of the square root of the treatment time at different temperatures. (□) 600° C, (◆) 650° C, (■) 700° C, (⊖) 800° C.

On the other hand, at 1000 and 1300° C the results were equivalent but very different from those at 800° C. Indeed, the ternary phase diagrams show (Fig. 11b) that for decreasing SiO_2 content in the initial mixtures, the following phases are successively observed to coexist: SiO_2–Ti_2O_3–Ti_5Si_3, Ti_2O_3–β-TiO–Ti_5Si_3, β-TiO–$TiO_{0.5}$–Ti_5Si_3, and finally α-Ti(O)–Ti_5Si_3.

Closely related results were obtained by thermodynamic calculations, based on Helmholtz energy minimization [16] between 700 and 1300° C, of the system Ti–SiO_2 [15], and taking into account the seventeen species given in Table III. In this case, the variation of the oxygen solubility in titanium was not considered, only the composition $x = 0.5$ corresponding to the boundary of the homogeneity range. Consequently, for SiO_2-poor mixtures, we found a region in which Ti_5Si_3 is in equilibrium with both Ti and $TiO_{0.5}$ (Fig. 11c), instead of the couples Ti_5Si_3–α-Ti(O).

The same results were obtained by starting from an initial system corresponding to the cement titanium and gaseous HCl with an important amount of silica including the substrate and the ampoule. We took an ampoule volume of $14\,cm^3$, Ti = 1.5×10^{-2} mol, HCl = 1.5×10^{-4} mol, and SiO_2 = 5 mol and calculated the equilibrium composition reached taking into account the previous species (Table III) and those given in Table IV. The thermodynamic data were tabulated previously [15, 17]. The equilibrium compositions resulting from the calculations performed between 700 and 1300° C were the same, showing that the phases in equilibrium with SiO_2 are always Ti_2O_3 and Ti_2Si_3 (Table V).

These results can be understood by considering that

TABLE III Thermodynamic calculations: species found in the Ti–Si–O system

Ti (s)	O_2 (g)	Ti_2O (s)
Ti (g)	α-TiO (s)	TiO (g)
Si (s)	TiO_2 rutile (s)	TiO_2 (s)
TiSi (s)	Ti_2O_3 (s)	SiO_2 (s)
$TiSi_2$ (s)	Ti_3O_5 (s)	SiO (g)
Ti_5Si_3 (s)	Ti_4O_7 (s)	

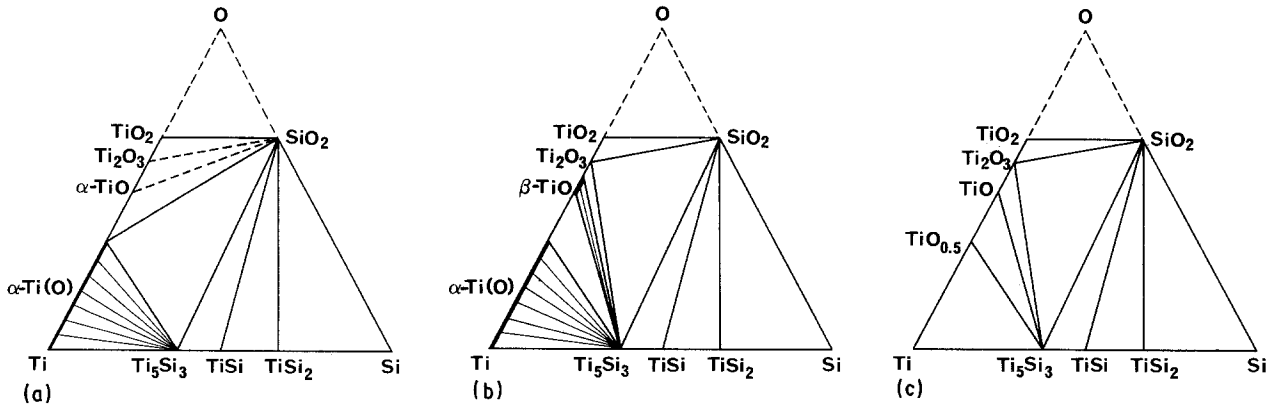

Figure 11 Ti–Si–O phase diagrams experimentally established at (a) 800° C, (b) 1000, (c) 1300° C, and calculated in the temperature range 700 to 1300° C.

at low reaction temperatures up to 800° C, kinetics factors impede the formation of phases that are thermodynamically stable, such as Ti_2O_3 or TiO. For that reason, metastable equilibria involving α-Ti(O), Ti_5Si_3 and SiO_2, which do not correspond to the lowest free energy of the system, are observed.

6. Discussion

In the Table V, we find in addition, H_2, $TiCl_4$ and $TiCl_3$ as gaseous species issuing from the reaction between hydrogen chloride and titanium [17]. The interactions between this gaseous phase of cementation and silica are similar to those observed between thin titanium films ranging from 30 to 600 nm and silica. This reaction has been investigated by several researchers using Rutherford backscattering spectroscopy [18–25], glancing angle X-ray diffraction [22] Auger microprobe analysis [23–25] and X-ray photoelectron spectroscopy [25]. They found that titanium slightly reacts with SiO_2 at about 500° C and that a strong interaction takes place above 600° C. A Ti_5Si_3 phase is in contact with SiO_2 while a Ti–O layer is at the surface of the sample. The composition of the top layer is well documented in the two more recent publications [24–25]. The O/Ti ratio is about 1.5 after annealing at about 800° C for 1 h and according to Morgan *et al.* [25], the oxide comprised TiO with a very thin zone of TiO_2 towards the surface. These results are in good agreement with our data obtained, in the case of thin amorphous coatings, either by XPS or LEEIXS analyses. In fact, this bilayer structure is observed whatever the total coating thickness. However, in the case of coatings thicker than 2 μm, that is crystalline coatings, the outer layer evidenced by XPS and LEEIXS, corresponds to TiO_x with $x \leqslant 0.5$, while the zone adjacent to the silica substrate is identified as Ti_5Si_3. In all cases, the Ti–SiO_2 interface is very reactive. Titanium atoms have a strong tendency to reduce neighbouring Si–O bonds to form Ti_5Si_3, while the oxygen liberated in this interaction reacts with titanium giving an oxide layer near the surface. This can explain the relatively sharp interface between Ti_5Si_3 and SiO_2, taking into account the process used to obtain the titanium-based coating. Moreover, from the presence of oxygen in Ti_5Si_3 and the formation of the Ti–O surface layer, it can be assumed that titanium and oxygen diffuse in opposite directions.

TABLE IV Thermodynamic calculations: species found in the Ti–H–Cl system

Cl (g)	TiCl (g)	H (g)
Cl_2 (g)	$TiCl_2$ (g)	H_2 (g)
$TiCl_2$ (s)	$TiCl_3$ (g)	TiH_2 (s)
$TiCl_3$ (s)	$TiCl_4$ (g)	HCl (g)

TABLE V Calculated equilibrium composition starting from the initial system: Ti = 1.5×10^{-2} mol, HCl = 1.5×10^{-4} mol, SiO_2 = 5 mol

Species	Mole numbers	Partial (atm) pressures
SiO_2	4.995	
Ti_2O_3	3.325×10^{-3}	
Ti_5Si_3	1.662×10^{-3}	
H_2 (g)	7.446×10^{-5}	0.425
$TiCl_4$ (g)	3.268×10^{-5}	0.186
$TiCl_3$ (g)	5.915×10^{-6}	0.034

7. Conclusion

We have developed a quite original procedure in a closed ampoule by which to coat silica surfaces with a titanium-based deposit, in the temperature range 600 to 800° C. The gaseous phase of cementation formed by the reaction between titanium and HCl, reacts with silica and a layer-by-layer growth takes place, which obeys a parabolic law. The resulting coatings thicker than 2 μm consist of a Ti_5Si_3 layer sandwiched between the substrate and an α-Ti(O) top layer.

The behaviour at elevated temperatures of the as-coated silica substrate embedded within an aluminium or a titanium matrix has also been studied. It is expected that the bilayer structure will play two functions: it will protect the silica from interactions with the metal, the inner phase Ti_5Si_3 being a good diffusion barrier, and it will allow a good adhesion of the substrate to the matrix, because of the outer Ti–O phase.

We will show, in a forthcoming paper, that using the cementation method, similar coatings are formed with alumina and mullite substrates.

References

1. B. GRANIER, C. CHATILLON and M. ALLIBERT, *J. Amer. Ceram. Soc.* **65** (1966) 465.
2. B. HOLMBERG, *Acta Chem. Scan.* **16** (1962) 1245.
3. J. L. MURRAY and H. A. WRIEDT, *Bull. Alloy Phase Diagrams*, **8** (1987) 148.

4. S. ANDERSON, U. KUYLENSTIERNA and A. MAGNELI, *Acta. Chem. Scand.* **11** (1957) 1641.
5. E. S. MAKAROV and L. M. KAZNETSOV, *J. Chem. Struct.* **1** (1960) 156.
6. S. YAMAGUCHI, *J. Phys. Soc. Jpn.* **27** (1969) 155.
7. *Idem, ibid.* **28** (1970) 1014.
8. R. J. WASILEWSKI, *Trans. Met. Soc. AIME* **221** (1961) 1231.
9. B. L. HENKE and E. S. EBISU, "Advances in X-ray Analysis", Vol. 17 (Plenum, New York, 1973) p. 150.
10. J. L. MURRAY, in "Binary Alloy Phase Diagrams", edited by T. B. Pratt (American Society for Metals, Ohio, 1986) p. 2054.
11. M. ROMAND, R. BADOR, M. CHARBONNIER and F. GAILLARD, *X-ray Spectrom.* **16** (1987) 7.
12. M. CHARBONNIER, M. ROMAND and F. GAILLARD, *Analysis* **16** (1988) 17.
13. W. L. BAUN, Air Force Materials Laboratory, Technical Report, AFMLTR 68161 (1968).
14. A. ROCHE, Thesis, Lyon (1983).
15. R. HILLEL, J. C. VIALA and J. P. SCHARFF, *Rev. Int. Hautes Tempr. Réfract. Fr.* submitted.
16. SGTE data bank "THERMODATA", Domaine Universitaire, Grenoble, France (1989).
17. R. HILLEL, J. C. VIALA and J. P. SCHARFF, *New J. Chem.* **13** (1989) 221.
18. H. KRAUTEL, M. A. NICOLET and J. W. MAYER, *Phys. Status Solidi* **20** (1973) K33.
19. *Idem, J. Appl. Phys.* **45** (1974) 3304.
20. R. PRETOREIUS, J. M. HARRIS and M. A. NICOLET, *Solid State Electron* **21** (1978) 667.
21. J. S. MAA, C. J. LIN, J. H. LIU and Y. C. LIU, *Thin Solid Films* **64** (1979) 439.
22. C. Y. TING, M. WITTMER, S. S. IYER and S. B. BRODSKY, *J. Electrochem. Soc.* **131** (1984) 2934.
23. L. J. BRILLSON, M. L. SLADE, H. W. RICHTER, H. VANDERPLAS and R. T. FULKS, *J. Vac. Sci. Technol.* **A4** (1986) 993.
24. A. E. T. KUIPER, M. F. C. WILLEMSEN and J. C. BARBOUR, *Appl. Surf. Sci.* **35** (1988–1989) 186.
25. A. E. MORGAN, E. K. BROADBENT, K. N. RITZ, D. K. SADANA and J. BURROW, *J. Appl. Phys.* **64** (1988) 344.

Received 3 March
and accepted 30 August 1989